ISSN 0030-400X, Optics and Spectroscopy, 2022, Vol. 130, No. 3, pp. 219–223. © Pleiades Publishing, Ltd., 2022.
Russian Text © The Author(s), 2022, published in Optika i Spektroskopiya, 2022, Vol. 130, No. 4, pp. 535–539.

Simulation of Gamma-Ray Generation in Interaction of High-Current Ultrarelativistic Particle Beams with Plasma

A. S. Samsonov[a], * and I. Yu. Kostyukov[a]

[a] *Institute of Applied Physics, Russian Academy of Sciences, Nizhny Novgorod, 603950 Russia*

**e-mail: asams@ipfran.ru*

Received December 20, 2021; revised December 20, 2021; accepted December 30, 2021

Abstract—Formation of hard photons in the process of interaction of high-current ultrarelativistic particle beams with extended plasma targets is analyzed. Dependence of conversion efficiency of beam energy to energy of gamma radiation on target parameters (thickness and density) is established using full-3D particle-in-cell simulation. An analytical estimate obtained within the framework of the approximate model agrees well with the results of numerical simulation. The studied interaction configuration can be a simple and efficient means of generating high-quality gamma beams.

Keywords: high-current beams, plasma targets, gamma radiation

DOI: 10.1134/S0030400X22030134

Studies in the area of strong-field physics are currently related mainly to using multi-petawatt laser facilities, such as ELI [1], SULF [2], Apollon [3], and 100-PW lasers (XCELS [4], SEL [5], etc.) in future. However, achieving higher and higher values of intensity imposes more and more strict requirements on contrast, stability, pulse quality, etc. [6]. In this regard, high-current particle accelerators that are characterized by high beam quality and stability can become an attractive alternative for experiments in the area of strong-field physics. Currently plasma methods of acceleration are considered to be a promising direction for creation of compact linear accelerators [7], e.g., the FACET-II project aims at construction of such an accelerator [8–10]. Charged-particle beams can generate strong electromagnetic fields in this kind of accelerators, which makes possible observing strong-field-physics processes, such as generation of gamma radiation in the process of nonlinear Compton scattering [11–13], creation of electron–positron pairs [14, 15], or even effects of nonperturbative quantum electrodynamics [9, 16, 17] upon collision of such beams with matter (or other beams).

It is expected that beams characterized by density of electrons exceeding 10^{29} m^{-3}, which corresponds to characteristic electron density in a solid, will be obtained at the FACET-II facility. A strongly nonlinear wave, or "bubble", can be driven in a solid upon propagation of such a beam, which formation is usually studied in much less dense media, e.g., gases [18, 19].

In the present work, we investigated the process of generation of gamma photons upon interaction of an ultrarelativistic electron beam with a thick plasma target by means of full-3D Particle-in-Cell (PIC) simulation. We analyzed the dependence of conversion efficiency of beam energy to energy of gamma rays on parameters of the target. Numerical simulation was carried out using the QUILL PIC code [20] in which formation of secondary particles was taken into account by using the Monte Carlo method. A hybrid scheme described in [21] that allows substantially reducing the growth rate of numerical Cherenkov instability [22–24] was used for numerical solution of Maxwell equations. Beam parameters were chosen close to those expected in the FACET-II facility: beam charge of 3 nC; average beam diameter and length of 400 nm and 1 μm, respectively; particle energy of 10 GeV. Target density was varied from 10^{27} to 5×10^{29} m^{-3}, while its thickness was varied from 1 to 100 μm. Beam interaction with more extended targets was not simulated in the present work, because various collisional (nuclear, Coulomb, etc.) processes that are not included in the QUILL code become essential in this case.

Results of simulation showed that beam propagation in the target is accompanied by formation of a cavity nearly completely free of electrons that propagates synchronously with the beam (Fig. 1). A quasi-static radial electric field and an azimuthal magnetic field in which beam particles perform betatron oscillations with a frequency equal to $\omega_{pl}/\sqrt{2\gamma}$, where plasma frequency ω_{pl} corresponds to unperturbed density of target electrons, and γ is the instantaneous value of the Lorentz factor of the particle, form in such strongly

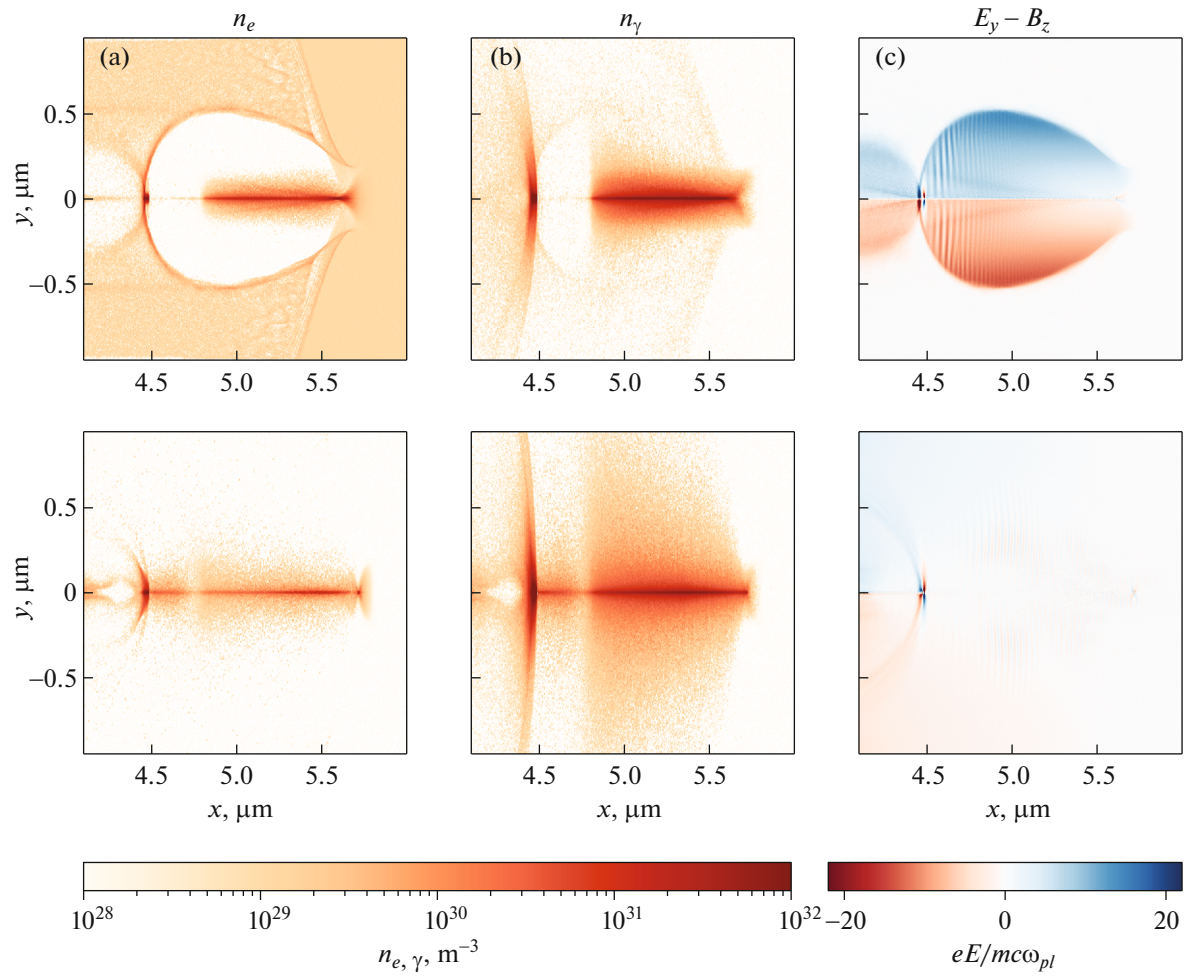

Fig. 1. (a) Distribution of electron density, (b) density of gamma photons, and (c) transverse force $E_y - B_z$ acting upon beam electrons in simulation of propagation of a high-current beam in a solid target with density $n_e = 10^{29}$ m^{-3} and thickness of 10 μm. The upper row corresponds to beam penetration into the target to a depth of 4 μm, while the lower row corresponds to the moment when the beam is exiting from the target.

nonlinear wake. In the process, radiation of electrons is incoherent and has synchrotron nature. Generated beam of gamma quanta reproduces spatial distribution of electrons and is characterized by a relatively low divergence. Gamma radiation has a broad spectrum with a cutoff at energy of initial electrons equal to 10 GeV that does not change in the process of interaction. In addition to radiative energy loss, beam electrons are slowed down by a longitudinal electric field generated in the plasma cavity. However, the latter effect is substantially weaker than the radiative energy loss for sufficiently dense targets. It is worth noting that formation of a "bubble" leads to the generation of a secondary electron beam in its trailing part, similar to the case of a rarified plasma. Electrons of this secondary beam are subjected to the action of an accelerating longitudinal field and also perform betatron oscillations thereby emitting radiation. Results of the simulation reveal that the cutoff energy of the secondary beam does not exceed 5 GeV, while the fraction of emitted energy does not exceed 15% relative to the total energy of gamma radiation.

Note that a similar scheme for generation of bright gamma beams based on collision of high-current ultrarelativistic particle beam with a series of thin metal films was proposed recently in [25]. In this configuration, an effective field acting upon beam electrons is formed as a result of "reflection" of the Coulomb field of the beam from a thin plasma layer and, in a sense, represents the field of transient radiation. Despite differences in physical mechanism of generation of gamma quanta, generation efficiency and spectrum of the output gamma radiation are very similar in the configuration used in [25] and in the configuration under consideration. According to the above discussion, beam electrons perform betatron oscillations in the field of a strongly nonlinear wake the structure of which is described in, e.g., [26]. Taking into account

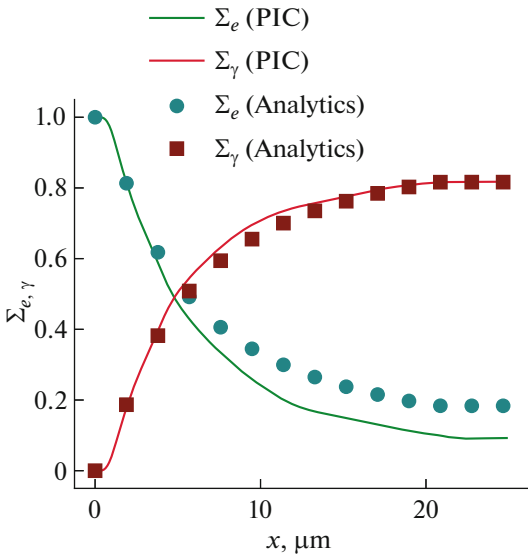

Fig. 2. Time dependence of total energy of electrons (Σ_e) and photons (Σ_γ) normalized to total initial energy of electrons. Solid lines represent the results of the QED-PIC simulation, while circles and squares represent an estimate obtained using expression (4) and numerical solution of equations (1) and (2).

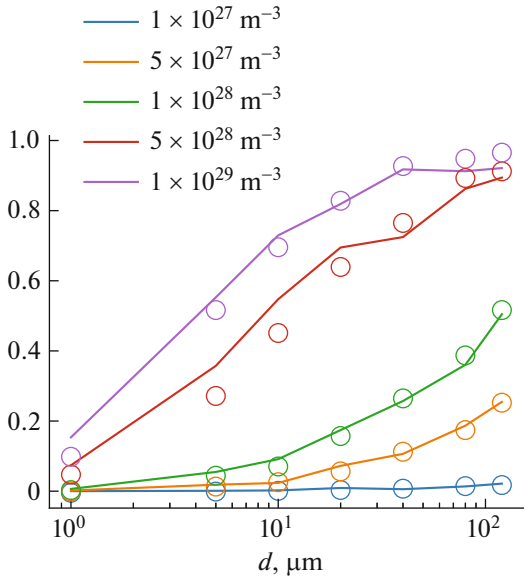

Fig. 3. Coefficient of conversion of electron-beam energy to energy of gamma radiation as a function of target density and thickness: solid lines—results of the QED-PIC simulation, symbols—analytical estimate (4).

radiation reaction in the quasi-classical approximation [27–31], equations of motion of electrons in such a wave averaged over a period of betatron oscillations have the form (detailed derivation of these equations can be found in, e.g., [32, 33])

$$\frac{d\rho}{dt} = -\frac{\rho}{\Gamma}\frac{1}{4\pi}\int_0^{2\pi} P\left(\frac{\rho\Gamma}{2a_S}|\cos\phi|\right)\sin^2\phi d\phi, \qquad (1)$$

$$\frac{d\Gamma}{dt} = -\frac{1}{2\pi}\int_0^{2\pi} P\left(\frac{\rho\Gamma}{2a_S}|\cos\phi|\right)d\phi, \qquad (2)$$

where ρ is the amplitude of betatron oscillations, Γ is the electron energy, and $a_S = m_e c^2/\hbar\omega_{pl}$. Normalization to plasma frequency ω_{pl} corresponding to unperturbed density of target electrons n_e is used in the above equations: time is normalized to $1/\omega_{pl}$, coordinates are normalized to c/ω_{pl}, momentum is normalized to mc, electromagnetic fields are normalized to $mc\omega_{pl}/e$, and power is normalized to $mc^2\omega_{pl}$. In the classical ($\chi_0 \ll 1$) and essentially quantum ($\chi_0 \gg 1$) cases, when power $P(\chi)$ of radiative losses is described by a power-law function of χ, the equations can be solved analytically:

$$\frac{\Gamma(t)}{\gamma_0} \approx \begin{cases}(1+0.625P(\chi_0)t/\gamma_0)^{-4/5}\\(1-0.149P(\chi_0)t/\gamma_0)^{24/5},\end{cases} \qquad (3)$$

where $\chi_0 = r_0\gamma_0/2a_S$, and r_0 is the initial deviation of an electron from the beam axis. Taking into account the number of particles located inside the target, we can finally find the time dependence of the total beam energy:

$$\Sigma_e(t) = \Sigma_0 - \int_{-2\sigma_x}^{0}\int_0^{r_b}(\gamma_0 - \gamma(x+ct))\eta(r,x) \times \Theta(x+ct)2\pi r dr dx, \qquad (4)$$

where $\Sigma_0 = N\gamma_0$, N is the number of electrons in the beam, function $\eta(x, r) = n_b(x, r)/N$ defines charge distribution in the beam, and $\Theta(x)$ is the Heaviside step function. An example of comparison of the latter estimate with the results of the QED-PIC simulation is presented in Figs. 2 and 3. Note that the discussed model does not take into account the presence of a longitudinal field in the plasma cavity that additionally slows down electrons. This circumstance explains the difference between an estimate of the beam energy obtained using expression (4) and its value obtained by numerical simulation.

Note that, with the beam parameters under consideration, efficiency of generation of electron–positron pairs from gamma quanta is too low to have an impact on the collision process even upon collision with a dense target. Therefore, formation of electron–positron pairs was not considered in detail in the present work.

Using full-3D numerical simulation, we thus discovered that two short bunches of gamma photons are

generated upon collision of a high-current ultrarelativistic electron beam with an extended solid target. The first bunch is related to radiation by electrons of the initial beam, while the second is caused by radiation of electrons injected into a plasma cavity created by the initial beam. In the process, conversion efficiency of electron-beam energy to energy of gamma photons can reach 90%. The studied scheme of generating gamma radiation is promising from the point of view of simplicity of its experimental realization and ultimately high efficiency.

FUNDING

This research was supported by the Russian Science Foundation, project no. 20-12-00077.

CONFLICT OF INTEREST

The authors declare that they have no conflicts of interest.

REFERENCES

1. The Extreme Light Infrastructure. https://www.eli-laser.eu.
2. Z. Gan, L. Yu, C. Wang, Y. Liu, Y. Xu, W. Li, S. Li, L. Yu, X. Wang, X. Liu, J. Chen, Y. Peng, L. Xu, B. Yao, X. Zhang, et al., in *Progress in Ultrafast Intense Laser Science XVI* (Springer, 2021), p. 199. https://doi.org/10.1007/978-3-030-75089-3_10
3. J. P. Zou, C. le Blanc, D. N. Papadopoulos, G. Chériaux, P. Georges, G. Mennerat, F. Druon, L. Lecherbourg, A. Pellegrina, P. Ramirez, F. Giambruno, A. Fréneaux, F. Leconte, D. Badarau, J. M. Boudenne, et al., High Power Laser Sci. Eng. **3** (e2) (2015). https://doi.org/10.1017/hpl.2014.41
4. XCELS. http://www.xcels.iapras.ru.
5. B. Shen, Z. Bu, J. Xu, T. Xu, L. Ji, R. Li, and Z. Xu, Plasma Phys. Control. Fusion **60**, 044002 (2018). https://doi.org/10.1088/1361-6587/aaa7fb
6. C. Danson, C. Haefner, J. Bromage, T. Butcher, J. F. Chanteloup, E. A. Chowdhury, A. Galvanauskas, L. A. Gizzi, J. Hein, D. I. Hillier, N. W. Hopps, Y. Kato, E. A. Khazanov, R. Kodama, G. Korn, et al., High Power Laser Sci. Eng. **7** (e54) (2019). https://doi.org/10.1017/hpl.2019.36
7. C. Schroeder, E. Esarey, C. Geddes, C. Benedetti, and W. Leemans, Phys. Rev. Accel. Beams **13**, 101301 (2010). https://doi.org/10.1103/physrevstab.13.101301
8. Technical Design Report for the FACET-II Project at SLAC National Accelerator Laboratory (2016). http://www.osti.gov/servlets/purl/1340171/.
9. V. Yakimenko, S. Meuren, F. del Gaudio, C. Baumann, A. Fedotov, F. Fiuza, T. Grismayer, M. Hogan, A. Pukhov, L. Silva, and G. White, Phys. Rev. Lett. **122**, 190404 (2019). https://doi.org/10.1103/PhysRevLett.122.190404
10. F. del Gaudio, T. Grismayer, R. Fonseca, W. Mori, and L. Silva, Phys. Rev. Accel. Beams **22**, 023402 (2019). https://doi.org/10.1103/PhysRevAccelBeams.22.023402
11. R. J. Noble, Nucl. Instrum. Methods Phys. Res., Sect. A **256**, 427 (1987). https://doi.org/10.1016/0168-9002(87)90284-1
12. R. Blankenbecler and S. D. Drell, Phys. Rev. D **36**, 277 (1987). https://doi.org/10.1103/PhysRevD.36.277
13. M. Bell and J. S. Bell, in *Quantum Mechanics, High Energy Physics Accelerators: Selected Papers of John S. Bell (With Commentary),* Ed. by M. Bell, K. Gottfried, and M. Veltman (World Scientific, 1995), p. 99. https://doi.org/10.1142/2611
14. P. Chen and V. I. Telnov, Phys. Rev. Lett. **63**, 1796 (1989). https://doi.org/10.1103/PhysRevLett.63.1796
15. J. Esberg, U. Uggerhøj, B. Dalena, and D. Schulte, Phys. Rev. Accel. Beams **17**, 051003 (2014). https://doi.org/10.1103/PhysRevSTAB.17.051003
16. M. Tamburini and S. Meuren, Phys. Rev. D **104**, L091903 (2020). https://doi.org/10.1103/PhysRevD.104.L091903
17. M. Filipovic, C. Baumann, A. M. Pukhov, A. S. Samsonov, and I. Yu. Kostyukov, Quantum Electron. **51**, 807 (2021). https://doi.org/10.1070/qel17606
18. J. Rosenzweig, B. Breizman, T. Katsouleas, and J. Su, Phys. Rev. A **44**, R6189 (1991). https://doi.org/10.1103/PhysRevA.44.R6189
19. A. Pukhov and J. Meyer-ter Vehn, Appl. Phys. B **74**, 355 (2002). https://doi.org/10.1007/s003400200795
20. QUILL Code. https://github.com/QUILL-PIC/Quill.
21. A. Samsonov, A. Pukhov, and I. Kostyukov, J. Phys.: Conf. Ser. **1692**, 012002 (2020). https://doi.org/10.1088/1742-6596/1692/1/012002
22. C. K. Birdsall and A. B. Langdon, *Plasma Physics via Computer Simulation* (CRC, Boca Raton, FL, 2004).
23. M. D. Meyers, C. K. Huang, Y. Zeng, S. A. Yi, and B. J. Albright, J. Comput. Phys. **297**, 565 (2015). https://doi.org/10.1016/j.jcp.2015.05.037
24. A. Blinne, D. Schinkel, S. Kuschel, N. Elkina, S. Rykovanov, and M. Zepf, Comput. Phys. Commun. **224**, 273 (2018). https://doi.org/10.1016/j.cpc.2017.10.010
25. A. Sampath, X. Davoine, S. Corde, L. Gremillet, M. Gilljohann, M. Sangal, C. Keitel, R. Ariniello, J. Cary, H. Ekerfelt, C. Emma, F. Fiuza, H. Fujii, M. Hogan, C. Joshi, et al., Phys. Rev. Lett. **126**, 064801 (2021). https://doi.org/10.1103/PhysRevLett.126.064801
26. I. Kostyukov, A. Pukhov, and S. Kiselev, Phys. Plasmas **11**, 5256 (2004). https://doi.org/10.1063/1.1799371

27. J. G. Kirk, A. Bell, and I. Arka, Plasma Phys. Control. Fusion **51**, 085008 (2009). https://doi.org/10.1088/0741-3335/51/8/085008

28. S. Bulanov, C. Schroeder, E. Esarey, and W. Leemans, Phys. Rev. A **87**, 062110 (2013). https://doi.org/10.1103/PhysRevA.87.062110

29. T. Z. Esirkepov, S. S. Bulanov, J. K. Koga, M. Kando, K. Kondo, N. N. Rosanov, G. Korn, and S. V. Bulanov, Phys. Lett. A **379**, 2044 (2015). https://doi.org/10.1016/j.physleta.2015.06.017

30. F. Niel, C. Riconda, F. Amiranoff, R. Duclous, and M. Grech, Phys. Rev. E **97**, 043209 (2018). https://doi.org/10.1103/physreve.97.043209

31. A. Gonoskov, T. Blackburn, M. Marklund, and S. Bulanov, arXiv: 2107.02161.

32. A. S. Samsonov, E. N. Nerush, I. Y. Kostyukov, M. Filipovic, C. Baumann, and A. Pukhov, New J. Phys. **23**, 103040 (2021). https://doi.org/10.1088/1367-2630/ac2e84

33. A. A. Golovanov, E. N. Nerush, and I. Yu. Kostyukov, New J. Phys. (2022). https://doi.org/10.1088/1367-2630/ac53b9